nature communications

Article

https://doi.org/10.1038/s41467-025-65148-6

Modeling and addressing on-target/off-tumor toxicity of claudin 18.2 targeted immunotherapies

Received: 20 November 2024

Accepted: 8 October 2025

Published online: 01 November 2025

Check for updates

Elizabeth J. Carstens[1,2,13], Kazuki Takahashi[1,2,3,13], Naoya Sakamoto[4,5,13], Martina De Vizio[1], Micaela Morgado[1], Shahryar Khoshtinat Nikkhoi[1], Abhishek Mangipudi[1], Canh Hiep Nguyen[1], Tate Weltzin[1], Izuma Nakayama[6], Qiang Lv[7], Jue Zeng[7], Cui Nie[7], Changjing Deng[7], Xiaoxiao Wang[7], Lile Liu[7], Samuel J. Klempner[8], Anusuya Ramasubramanian[1], Jonathan A. Nowak[9,10], Andrew J. Aguirre[1,2,3,9,14], Kohei Shitara[6,11,14] & Eric L. Smith[1,2,12,14]

Successfully extending immunotherapies to solid tumors involves addressing several key challenges, importantly the "antigen dilemma", the expression of a solid tumor target antigen on the normal tissue of tumor origin. Claudin 18.2 (CLDN18.2) has emerged as an important target for upper gastrointestinal (GI) cancer therapies (such as Zolbetuximab, a naked antibody, recently approved; or CT041, a second-generation chimeric antigen receptor (CAR) T cell therapy with promising clinical data). However, GI toxicities are reported from clinical use of both Zolbetuximab and CT041. Here, we describe clinical Zolbetuximab treatment associated cases of gastric erosive lesions. We also demonstrate and characterize on-target/off-tumor gastric toxicity targeting CLDN18.2 in a pre-clinical mouse model of CT041-scFv derived CAR T cell therapy. By developing CLDN18.2 fully-human VH-only single domain CARs, we demonstrate that on-target/off-tumor toxicity inversely correlates with affinity of the binder, and that a lower affinity CAR may widen the therapeutic window for CLDN18.2 by decreasing on-target/off-tumor toxicity while preserving efficacy.

Globally, gastric cancer has the fifth highest incidence and mortality of any malignancy[1,2]. A large portion of patients present with de novo advanced disease, and over 50% of patients with locoregional disease will develop recurrent metastatic disease. While biomarker-selected strategies are increasingly driving frontline management, the median overall survival (mOS) for advanced disease is 14–17 months[3–5]. Standard biomarker testing includes assessment of PD-L1 expression, HER2 expression and/or amplification, and mismatch repair or microsatellite instability testing and, more recently, claudin 18.2 (CLDN18.2) testing. On average, these strategies improve survival by roughly 2–4 months versus chemotherapy alone, and managing toxicities that impact quality of life is central to optimizing patient outcomes.

[1]Department of Medical Oncology, Dana-Farber Cancer Institute, Boston, MA, USA. [2]Harvard Medical School, Boston, MA, USA. [3]The Broad Institute of Harvard and MIT, Cambridge, MA, USA. [4]Department of Pathology and Clinical Laboratories, National Cancer Center Hospital East, Kashiwa, Japan. [5]Division of Pathology, Exploratory Oncology Research and Clinical Research Center, Kashiwa, Japan. [6]Department of Gastroenterology and Gastrointestinal Oncology, National Cancer Center Hospital East, Kashiwa, Japan. [7]Nona Biosciences (Suzhou) Co., Ltd, Suzhou, China. [8]Department of Medicine, Division of Hematology–Oncology, Massachusetts General Hospital, Boston, MA, USA. [9]Department of Medicine, Brigham and Women's Hospital, Boston, MA, USA. [10]Department of Pathology, Brigham and Women's Hospital, Boston, MA, USA. [11]Department of Immunology, Nagoya University Graduate School of Medicine, Nagoya, Japan. [12]Parker Institute for Cancer Immunotherapy, Dana-Farber Cancer Institute, Boston, MA, USA. [13]These authors contributed equally: Elizabeth J. Carstens, Kazuki Takahashi, Naoya Sakamoto. [14]These authors jointly supervised this work: Andrew J. Aguirre Kohei Shitara, Eric L. Smith.
e-mail: ericl_smith@dfci.harvard.edu

The CLDN18.2 isoform has been identified as a target of interest given its high prevalence in both primary lesions and metastases of upper gastrointestinal cancers[6–9]. Claudin 18 (CLDN18) belongs to a group of transmembrane proteins participating in tight junctions. It has two isoforms, CLDN18.1, primarily restricted to the lung, and CLDN18.2, which in normal tissues is limited to the differentiated epithelial cells of the stomach[10]. CLDN18.2 was detected by IHC in almost 80% of primary gastric adenocarcinomas, and the majority of cases investigated showed similar staining patterns between primary and involved lymph nodes[11]. In addition to expression in gastric adenocarcinoma, CLDN18.2 has been detected in pancreatic, esophageal cancer, ovarian, and a limited number of non-small cell lung cancers[12–15].

The limited normal tissue expression and distribution coupled to the high prevalence of tumor expression (inherent tumor specificity) made CLDN18.2 an attractive therapeutic target. Following promising phase II data, the chimeric IgG1 antibody zolbetuximab (formerly IMAB-362) entered two parallel phase III trials (GLOW, SPOTLIGHT) in CLDN18.2+ gastroesophageal cancers[16,17]. A combined analysis of both trials showed that the addition of zolbetuximab to first-line chemotherapy resulted in significantly longer progression-free survival (PFS) and overall survival (OS) compared to chemotherapy alone, leading to global regulatory approvals in 2024[18]. Following the success of zolbetuximab, numerous CLDN18.2-directed strategies are actively being explored in the clinic[19]. Antibody drug conjugates are under clinical development[20], and CAR T cell therapies have also joined the armamentarium with the CLDN18.2-targeted CAR T cell therapy, CT041 (Satri-cel). In gastric and pancreatic cancer, CT041 has demonstrated an encouraging efficacy signal, with an overall response rate of 38.8% and median PFS (mPFS) of 4.4 months in a single-arm study; and in a randomized study of heavily pre-treated gastric cancer, mPFS of 3.25 months, comparing favorably to the physicians' choice control arm (mPFS 1.77 months). While modest, this is one of the first CAR T cell therapies for solid tumors with unequivocal clinical anti-tumor efficacy in a clinical setting with enormous unmet need[21–23].

In the trials of both zolbetuximab and CT041, some of the most common treatment-emergent adverse events (not expected to be related to required co-administered chemotherapy) were nausea and vomiting. Nausea was seen in 76.0% of the patients who received zolbetuximab and chemotherapy and in 56.2% of those who received chemotherapy with a placebo. Vomiting occurred in 66.8% and 34.2%, respectively. Around 30% of patients in these trials had been previously treated with gastrectomy, and both gastrointestinal (GI)-related toxicities were more likely to occur in patients with intact stomachs. CT041-treated patients also experienced high rates of gastrointestinal toxicity, with any grade GI disorder occurring in 92% of patients, including 20% of patients with ≥grade 3 toxicity. Nausea and vomiting occurred in 67% and 53% of patients, respectively. Gastric mucosa injury (which included gastritis, erosive gastritis, and mucosal lesions) was reported in 8.2% of patients. Additional reports of GI hemorrhage and perforation were also made[21]. Of note, the overall rate of prior gastrectomy in this trial is unknown. Another CLDN18.2-targeted CAR (LB1908) presented first-in-human data on a small initial cohort of patients. This trial reported 50% grade ≧3 "gastritis/gastric mucosal injury," including a dose-limiting toxicity (DLT)[24]. The mechanism of CLDN18.2 therapy-related nausea, vomiting, gastritis, and other GI injuries is hypothesized to involve off-tumor/on-target binding to normal CLDN18.2 expressed in gastric epithelium; however, these clinical observations call into question the idea that CLDN18.2's role in tight junctions excludes access by immunotherapies and is completely protective. Given this, and the rapid expansion of the therapeutic landscape, an understanding of the pathological injury in human samples and pre-clinical models that can approximate the therapeutic window of experimental agents represents a current clinical and scientific knowledge gap.

Here, we report on the clinical and pathological rates of gastric mucosal injury in patients treated with zolbetuximab as standard of care and describe a pre-clinical model validating the on-target/off-tumor GI toxicity of CLDN18.2-directed CAR T cell therapies. Gastric-specific isoform 18.2 is distinguished from the lung-specific isoform 18.1 by its inclusion of exon 1b (rather than 1a), and isoform-specific binders interact with this region[25]. Amino acid sequences from mouse and human exon 1b have 97% identity. Taking advantage of this homology between mouse and human CLDN18.2 (Supplementary Fig. 1), we study CLDN18.2 CAR T cell therapy, using the binder from CT041, to demonstrate pathological injury that matches the on-target/off-tumor toxicity that we observe in zolbetuximab-treated patients. We additionally develop fully-human VH-only binders to CLDN18.2, which, when engineered into a CAR T cell therapy, induce less on-target/off-tumor toxicity while still maintaining anti-tumor efficacy, thus potentially improving the therapeutic window in this important class of cell therapies.

Results

Clinically significant erosive gastritis from on-target/off-tumor activity targeting CLDN18.2

To better understand potential histopathologic correlates to the high rates of nausea and vomiting in non-gastrectomy patients treated with zolbetuximab plus chemotherapy, 50 out of 58 sequentially treated patients underwent paired pre- and on-treatment upper endoscopy (EGD) during standard therapy. Among the 58 zolbetuximab-treated patients for whom EGD was performed, we observed that 52 (90%) of these showed endoscopic changes to their gastric mucosa, including redness, erosion, and/or superficial ulcers, which were consistent with findings suggestive of gastritis. Amongst this cohort, 41 were male and 17 female, with 37 and 15 patients developing gastritis, respectively; thus, there was no statistically significant difference in gastritis by sex. Examples are provided, where prior to treatment, endoscopy demonstrated normal mucosa (Fig. 1A, Supplementary Fig. 2A–D), while EGD on-treatment showed grossly visible gastritis (Fig. 1B, Supplementary Fig. 2E–H). In one patient example, endoscopic tissue sampling of the tumor-uninvolved gastric epithelium was performed before (Fig. 1C, D) and after (Fig. 1E, F) treatment with four doses of zolbetuximab and chemotherapy. Samples from this patient were stained for CLDN18.2 expression using the approved 43-14A anti-CLDN18.2 antibody clone (Roche Ventana, Oro Valley, AZ). Follow-up biopsies demonstrated erosive gastritis, denuded normal architecture, and preserved CLDN18.2 expression (Fig. 1E, F). Notably, all patients with gastritis were able to continue zolbetuximab-based therapy; patients with follow-up EGD at the time of progressive disease often showed improvement in gastric injury (Supplementary Fig. 2I–L).

Pre-clinical model of CLDN18.2-targeted CAR T cell therapy using the same scFv binder as CT041 reproduces on-target/off-tumor toxicity

To evaluate the efficacy and toxicity profile of CAR T cell therapy targeting CLDN18.2, we engineered a CAR utilizing the scFv sequence from CT041[26]. We investigated a second-generation CAR design incorporating the CT041-scFv, a 4-1BB co-stimulatory domain, and a CD3ζ activation domain. To evaluate this construct in vivo, we employed NSG-MHC class I/II double knock out mice (NSG-DKO), which protects mice from potentially confounding human T cell-mediated xenogeneic graft vs host disease[27]. Animals were subcutaneously engrafted with OE19 cell line, which endogenously expresses CLDN18.2 and was derived from a human gastric cardia/gastroesophageal junction adenocarcinoma. CT041-scFv CAR T cells and irrelevantly targeted BCMA-scFv human CAR T cells (dose: 1×10^6 CAR+ cells) were evaluated in mice bearing tumors with an average size of ~100 mm^3. Tumors in animals treated with CT041-scFv CAR T cells regressed (Fig. 2A); however, animals rapidly succumbed to weight

https://doi.org/10.1038/s41467-025-65148-6

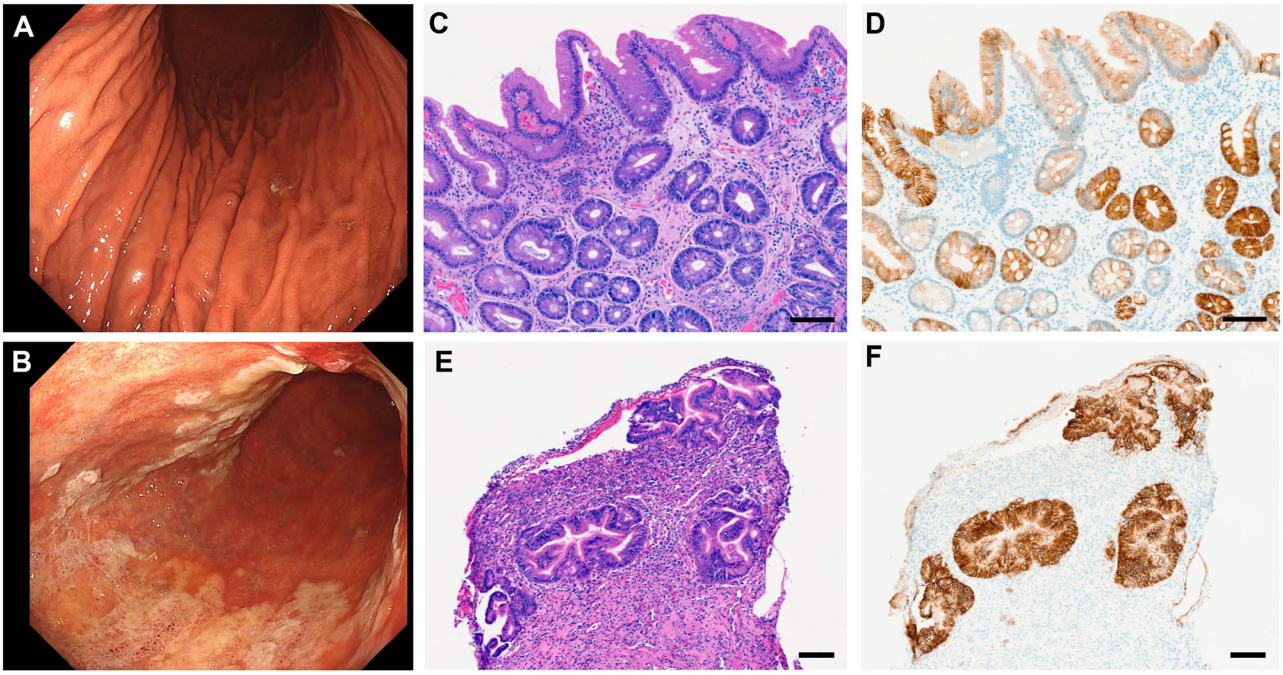

Fig. 1 | Erosive gastritis after zolbetuximab. A Pre-treatment endoscopic image in a gastric cancer patient, from a cohort of $n = 58$ patients. **B** After four doses of zolbetuximab plus chemotherapy, follow-up endoscopy shows grossly visible gastric mucosal injury. **C**, **D** H&E and IHC from biopsies of tumor-uninvolved gastric epithelium, taken prior to treatment, demonstrate strong CLDN18.2 (43-14A clone) expression (magnification at 4×). Scale bars are 100 µm. **E**, **F** Biopsies from tumor-uninvolved gastric epithelium post-treatment demonstrate erosive gastritis with regenerative changes and preserved CLDN18.2 expression (magnification at 4×). Scale bars are 100 µm. Biopsy and pathology were performed on $n = 48$ patients. Micrographs representative of CLDN18.2-positive gastritis from this cohort.

loss and failure to thrive (Fig. 2B, C). In control mice, treated with either BCMA-scFv CAR T cells or no cell injection, all tumors progressed, and there was no evidence of toxicity from treatment. Animals were sacrificed when they reached the endpoint due to either toxicity or tumor progression, and stomach tissues were collected. Sections of stomachs from these animals were stained with hematoxylin and eosin (H&E) and multiplex immunofluorescence (mIF) for the presence of CLDN18.2 and human CD3 to identify T cell infiltration. Animals treated with CT041-scFv CAR T cells show atrophy and disrupted stomach architecture on H&E (Fig. 2D). Sections clearly show the presence of CLDN18.2 (Fig. 2E) and dense T cell infiltration (Fig. 2F) into the stomach tissue. Any remaining tumor from treated animals was also collected. While scant tumor remained in CT041-scFv treated animals at the time of sacrifice (Supplementary Fig. 3A, B), CDLN18.2-positive tumor cells were identified (Supplementary Fig. 3C), surrounded also by a dense human T cell infiltrate (Supplementary Fig. 3D–F). In irrelevantly targeted CAR T cell control-treated animals, normal stomach architecture is preserved (Supplementary Fig. 3G, H). While CLDN18.2 is clearly present in these stomach sections as well (Supplementary Fig. 3I), there is no corresponding T cell infiltrate (Supplementary Fig. 3J–L).

On-target/off-tumor toxicity is independent of tumor burden, but demonstrates dose dependence, without a sufficient therapeutic window

To investigate if excess antigen from a large tumor burden drove toxicity, we developed an experimental approach where a tumor was established in two cohorts of mice, 1 week apart. These two cohorts of mice, high burden (~200 mm^3) and low burden (~100 mm^3) groups and a third tumor-free cohort, were injected with 1×10^6 CT041-scFv CAR+ T cells on the same day (Fig. 3A). While tumor-bearing animals again showed almost complete clearance of tumor, regardless of tumor burden (Fig. 3B), all CT041-scFv CAR T cell-treated animals lost substantial body weight (Fig. 3C) and reached humane endpoint within 22 days. Ultimately, irrespective of tumor burden, survival was no longer for CT041-scFv CAR T cell-treated mice, limited by toxicity, than for control animals treated with irrelevantly targeted CAR T cells, where survival was limited by lack of tumor control (Fig. 3D, E). Data representative of two models with distinct tumor types (OE19, PATU8998s). Dense T cell infiltration at the stomach is present regardless of whether a tumor is present or not (Supplementary Fig. 4). Clinically, CLDN18.2 expression can be upregulated or downregulated in gastric loss of membrane polarization as compared to stomach adenocarcinomas relative to endogenous expression levels, where downregulation may even correlate with development, infiltration and proliferation; the malignant transformation also alters the localization of CLDN18.2[28]. These clinical findings were observed here, with tumor samples showing reduced expression of CLDN18.2 and loss of membrane polarization as compared to the stomach. In the normal murine gastric mucosa, CLDN18.2 was uniformly expressed in differentiated epithelial cells and was enriched at the basolateral cell membrane. In contrast, in tumor cells CLDN18.2 expression was more heterogeneous, where it was expressed at a lower intensity than normal gastric mucosa, and exhibited membranous and cytoplasmic subcellular expression without basolateral enrichment, suggesting loss of membrane polarization more consistent with non-junctional staining (Supplementary Fig. 5).

To test whether CAR T cell dose modulates the severity of toxicity, animals were engrafted with OE19; when tumors reached 200 mm^3 they were treated with a narrow dose de-escalation of CT041-scFV CAR T cells (starting with the commonly used xenograft model dose 1×10^6 and continuing with more clinically relevant weight-based doses 3×10^5, and 1×10^5). In contrast to the results observed with tumor burden, CAR T cell number impacted both toxicity and efficacy in a clear dose-dependent manner. Animals treated with lower doses had less body weight loss (Fig. 3F), but also had less effective tumor clearance (Fig. 3G). Throughout this narrow dose de-escalation, while lower doses showed some benefit, the tradeoff between anti-tumor

https://doi.org/10.1038/s41467-025-65148-6

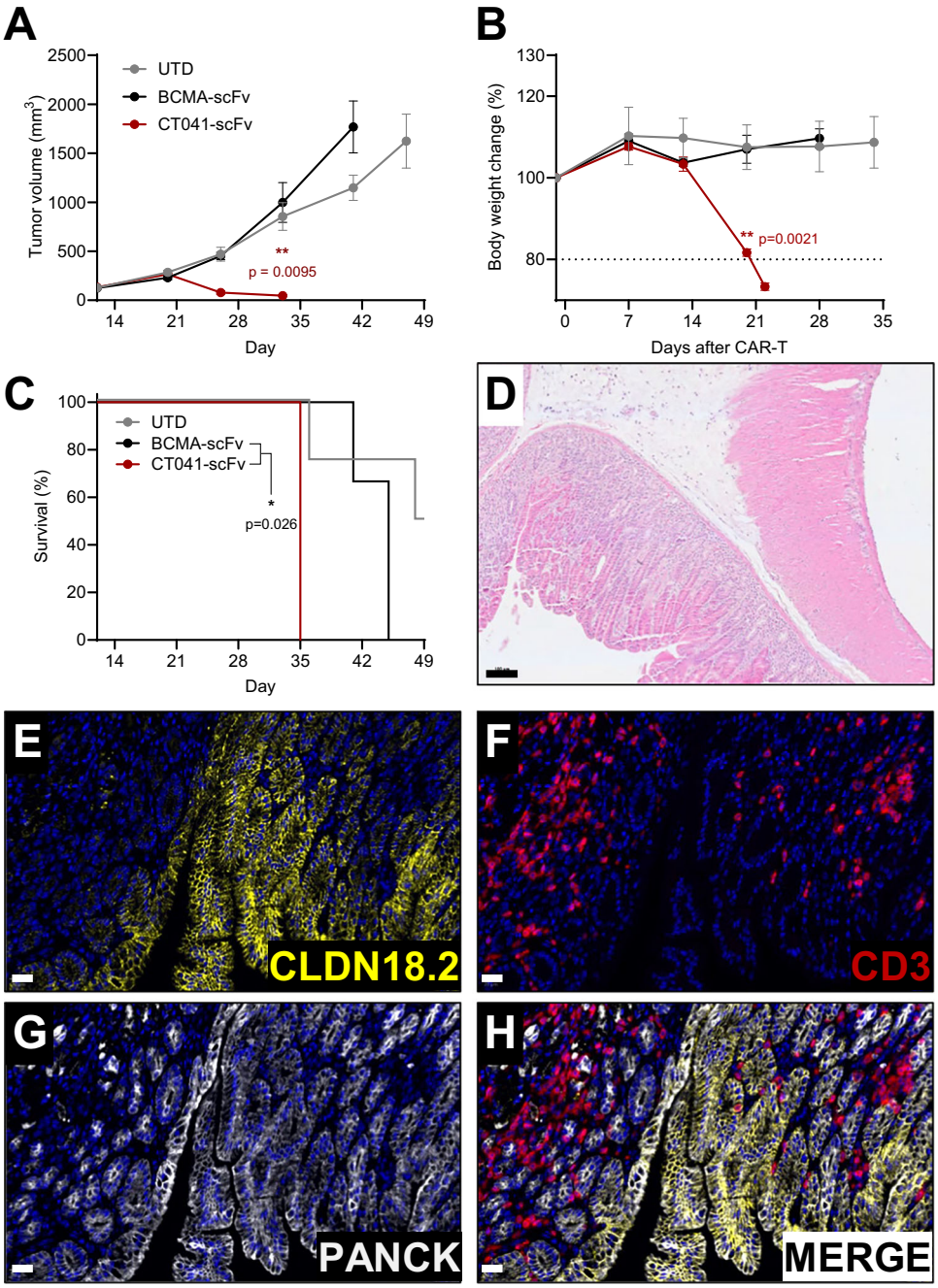

Fig. 2 | Treatment with CT041-scFv CLDN18.2-targeted CAR T cells leads to intolerable on-target/off-tumor toxicity. NSG-DKO mice bearing OE19 xenografts were left untreated (UTD, $n = 4$) or treated on day 13 with 1×10^6 CT041-scFv ($n = 4$) or BCMA-scFv ($n = 3$) CAR T by tail vein. **A** Tumor volume over time, comparing BCMA-scFv and CT041-scFv CAR treatment. Data are presented as mean ± SEM. **B** Body weight, comparing BCMA-scFv and CT041-scFv. Animals reached humane endpoint if body weight declined by 20% or due to tumor progression. Data are presented as mean ± SEM. **C** Overall survival. **D** Stomach from a CT041-scFv-treated animal at the time of sacrifice due to toxicity. H&E shows atrophy of normal architecture and inflammation (scale bar 100 μm). **E**–**H** Tissue was stained via immunofluorescence for **E** CLDN18.2, **F** human CD3, **G** epithelial marker, PANCK. DAPI identifies cell nuclei (blue). **H** Merge demonstrates strong gastric CLDN18.2 expression with colocalization of human CD3+ T cells. Scale bars 20 μm. **D**–**H** representative of $n = 2$ mice. **A**, **B** unpaired, two-sided t-test. **C** Log-rank Mantel–Cox test, $^*p < 0.05$; $^{**}p < 0.01$.

efficacy and on-target/off-tumor toxicity limited improvement in OS (Fig. 3H). Consistent with this, examining tumor vs non-tumor related mortality as visualized with a swimmers plot, shows that the majority of animals at the higher 3×10^5–1×10^6 doses succumb to toxicity, while animals treated with the lowest dose, 1×10^5 CAR T cells, show less toxicity, but ultimately less durable tumor control, as all but one animal ultimately succumbed to tumor progression prior to Day 100 (Fig. 3I).

A VH-only binder with lower affinity mitigates on-target/off-tumor toxicity while preserving anti-tumor efficacy

In order to determine if the therapeutic window targeting CLDN18.2 could be enhanced with CAR T cells utilizing alternative binders, a fully-human heavy chain only antibody (HCAb) discovery campaign was conducted. Briefly, transgenic mice knocked out for murine variable heavy and light (VH/VL) chain loci and knocked in for only the human VH chain locus (HCAb mice[29]) were immunized with HEK293

https://doi.org/10.1038/s41467-025-65148-6

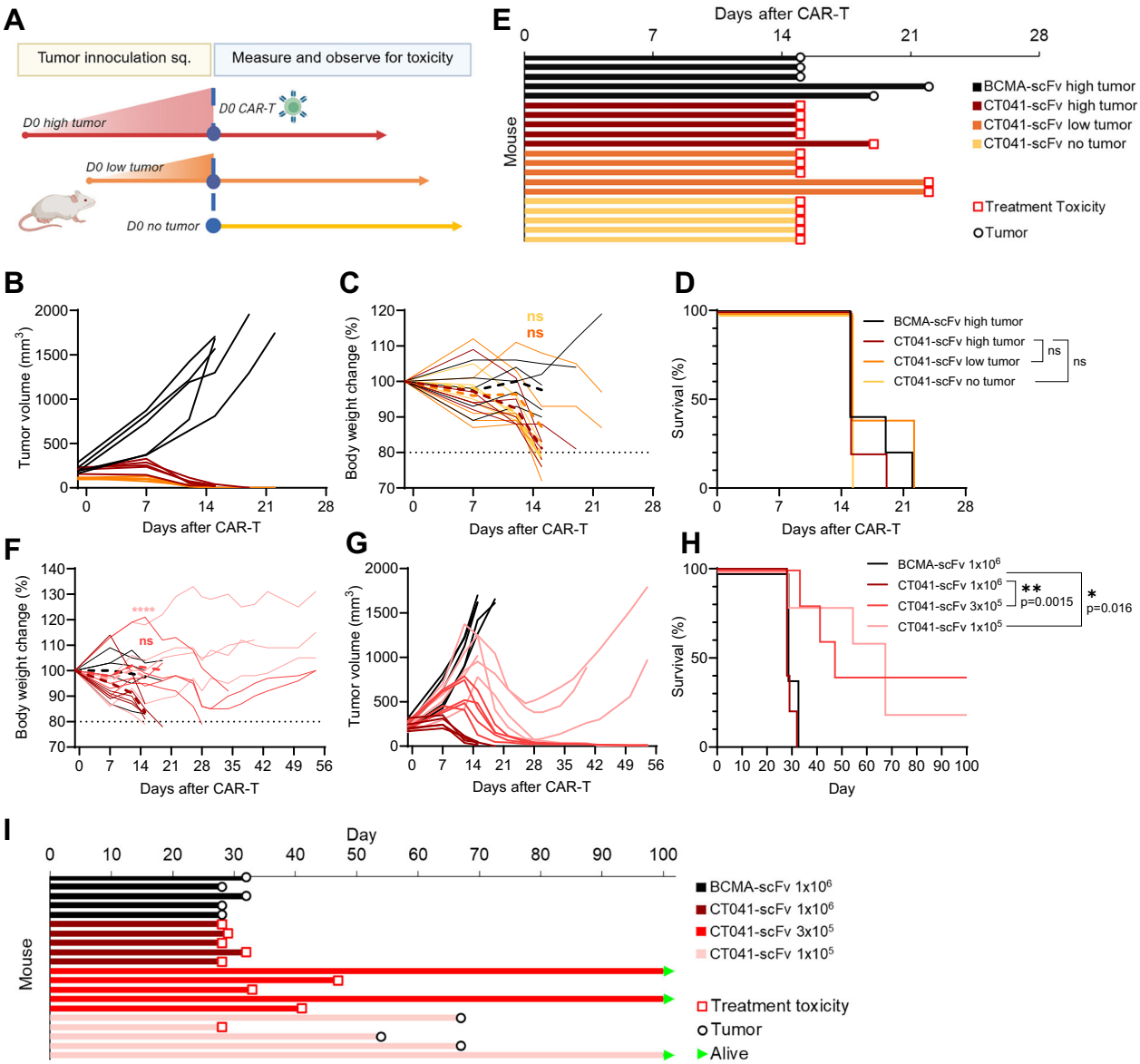

Fig. 3 | Toxicity from CT041-scFv is dependent on dose and not tumor burden. **A** Experimental schematic of B-E indicating the injection of OE19 xenografts subcutaneously, staggered such that animals were treated with CAR T cells once tumors reached ~100 mm^3 or ~200 mm^3, to model low or high burden disease. Non-tumor-bearing animals were also treated. All animals received 1×10^6 CT041-scFv or BCMA-scFv CAR T cells by tail vein. Created in BioRender. Haggerty, T. (2025) https://BioRender.com/zhyrglg. **B** Tumor volume and **C** spider plot of individual mouse body weight changes (solid lines) with mean overlay (dashed lines), significance shown relative to high tumor cohort, two-way ANOVA. **D** Overall survival (Log-rank Mantel–Cox test). $n = 5$ mice/group, **E** Individual cause of death is shown as a swimmers plot. **F**–**I** Female NSG-DKO mice were engrafted with OE19 subcutaneously and dosed by tail vein with either 1×10^5, 3×10^5, or 1×10^6 CT041-scFv or 1×10^6 BCMA-scFv CAR T after tumor volume had reached 200 mm^3 on day 13. This was replicated in an independent experiment with male mice. **F** Spider plot of body weight (solid line), with mean overlay (dashed lines), significance shown relative to 1×10^6 dose, two-way ANOVA (**G**) tumor volume. **H** Overall survival (Log-rank Mantel–Cox) $n = 5$ mice/group. **I** Individual cause of death is shown in swimmers plot. Green arrowheads: animals still alive at the end of the experiment; red squares: succumb to toxicity; black circle: succumb to tumor. Tumor volumes and body weights were measured weekly. $^*p < 0.05$, $^{**}p < 0.01$, and $^{****}p < 0.0001$, ns non significant.

cells overexpressing recombinant human CLDN18.2, and binders were obtained through Single B Cell screening on the Beacon Optofluidic system and subsequent VDJ sequencing. From this HCAb discovery campaign, two highly active and specific binders, "5795" and "5797," were identified and cloned into the same 4-1BB/CD3ζ containing second-generation CAR construct, hereafter called "5795-VH" and "5797-VH." Multicycle kinetics for each bivalent linked, IgG-reformatted binder against human CLDN18.2 were assessed by surface plasmon resonance (SPR), revealing a 10-fold range of affinities for the binding elements within the three CARs. CT041 IgG had the highest affinity with a K_D of 3.64 ± 0.2 nM; 5797-IgG had a slightly lower affinity of 4.5 ± 3 nM, while 5795-IgG had the lowest affinity of 21.8 ± 2 nM (Fig. 4A; Supplementary Fig. 6A–C). Affinity of each binder to mouse claudin 18.2 is similar to human claudin 18.2 and follows this same trend (Supplementary Fig. 6D–F). We further characterize the binding epitope within human claudin 18.2. Taking advantage of the non-binding CLDN18.1 isoform, structurally proximate residues that differed between isoform 18.1 and 18.2 were mutated to those found in CLDN18.1, resulting in three chimeric 18.1/18.2 constructs. Cell lines bearing these chimeric constructs were then subjected to killing by 5795, 5797-VH, and CT041-scFv CAR T in vitro. While all CAR candidates require wild-type ECL1-2 and ECL1-3 residues, the VH binder-

https://doi.org/10.1038/s41467-025-65148-6

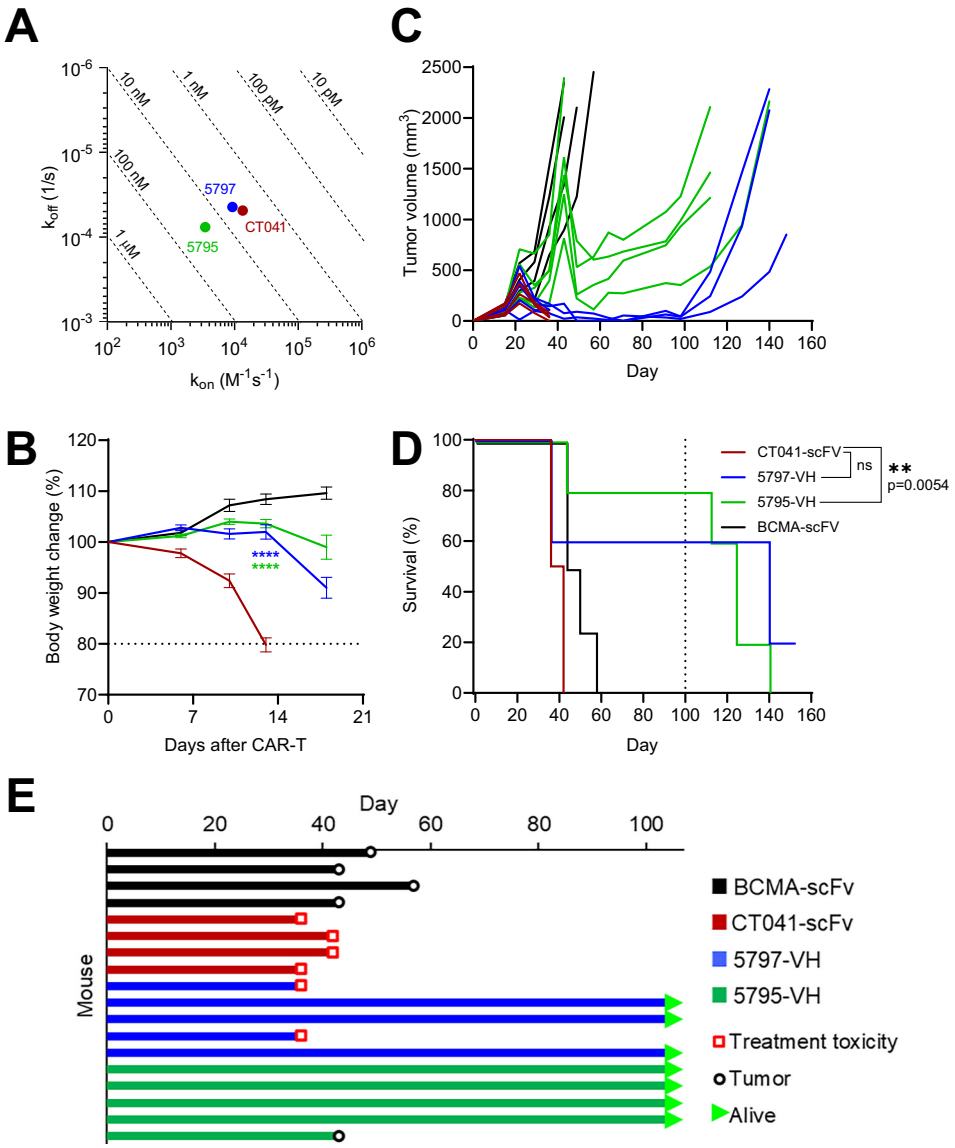

Fig. 4 | Binding affinity correlates with on-target/off-tumor toxicity. Binding affinity, as measured by multicycle kinetics, of bivalent VH-Fcs targeting human CLDN18.2, and that of CT041-scFv-Fc. **A** Iso-affinity plot of binders (from SPR data in Supplementary Fig. 6, $n = 3$). **B** NSG-DKO animals were administered CLDN18.2-targeted VH CAR T cells, CT041-scFv CAR T cells, or BCMA-scFv CAR T cells, and body weight was measured weekly (two-way ANOVA, relative to CT041-scFv). $n = 5$ mice/group. Data are presented as mean ± SEM. **C**–**E** NSG-DKO animals were injected with OE19, treated with CAR T cells as in B on day 16, and followed for **C** tumor control and **D** overall survival, Log-rank Mantel–Cox. $n = 4$ mice received CT041-scFv or BCMA-scFv CAR T, $n = 5$ mice received 5795-VH or 5797-VH CAR T. **E** Swimmers plot shows the cause of death. The OE19 gastric cancer study data are representative of two independent experiments in male and female mice. $^{**}p < 0.01$, $^{****}p < 0.0001$, ns non significant.

based CARs additionally rely more heavily on interactions with ECL1-1 residues than CT041. In contrast, CT041-scFv CAR T were able to kill cells expressing chimeric CLDN18.2 harboring 18.1 residues in ECL1-1, indicating less activity-dependent binding at this site (Supplementary Fig. 7A, B).

These candidates were then screened in vivo for toxicity. Mice were injected with 1×10^6 CLDN18.2 VH, CT041-scFv CAR T cells, or irrelevantly targeted (BCMA-scFv) CAR T cells. Toxicity, as assessed by weight loss, was seen in the CLDN18.2-targeted arms proportionally to the binding affinity of the binder within the CAR construct (Fig. 4B). Next, binders were tested in vivo for efficacy. As before, animals were engrafted with OE19 and treated with 1×10^6 CAR T cell dose. Nearly all animals treated with CLDN18.2-targeted CAR T cell therapy showed an anti-tumor response (Fig. 4C) compared to BCMA-treated controls. As expected, however, animals treated with CT041-scFv CAR T cells all lost weight and required sacrifice due to toxicity, substantially limiting survival extension. Animals treated with the similar affinity 5797-VH CAR T cells also showed some toxicity requiring euthanasia, but the remaining animals showed long-term tumor control. Animals treated with 5795-VH CAR T cells, however, were the only group to completely escape early toxicity requiring sacrifice, with most animals exhibiting initial tumor clearance and significantly prolonged mOS relative to CT041-scFv-treated animals (CT041-scFv mOS 39 days vs 5795-VH mOS 124 days $p < 0.001$), despite ultimately having tumor recurrence (Fig. 4D, E).

We also investigated the therapeutic window across these CARs in a pancreatic cancer xenograft model, PATU8988s (Supplementary Fig. 8A–D). Tumors were allowed to engraft and expand for 2 weeks when NSG-DKO mice were treated with a single dose of either 3×10^5 or 1×10^6 5795-VH, 5797-VH, or CT041-scFv CAR T and compared 1×10^6 BCMA-scFv irrelevantly targeted control-treated animals. All animals treated with either CT041 or 5797-based CAR T succumbed to toxicity,

even at the lower dose, while 5795-based CAR T had long-term tumor control at both doses, with minimal toxicity in this tumor model (mOS 31–36 days for CT041-scFv groups and mOS not reached by 60 days for 5795-VH groups; $p < 0.01$). The stomach was harvested from animals in this model, with the CT041-scFv CAR showing the highest degree of CAR T cell infiltration into the stomach and the 5795-VH CAR T showing the lowest (Supplementary Fig. 9A–H). This also correlated with the degree of tissue disruption, with almost complete atrophy and erosion in the CT041-scFv treated group, only around 1% atrophy and some erosion in the 5797-VH treated animal, very little, if any tissue disruption in the 5795-VH animal, and normal stomach architecture in the BCMA-scFv control (Supplementary Fig. 9I–L).

In summary, these data in both humans and animal models demonstrate that CLDN18.2 targeting can result in meaningful toxicity, likely due to on-target/off-tumor toxicity within the gastric epithelium. While we observed dose dependence to this toxicity that was independent of tumor burden, we also found that toxicity and efficacy can be balanced through careful selection of binders and in vivo toxicity evaluation.

Discussion

CLDN18.2-targeted therapies have the potential to have a profound impact on the treatment of several solid tumors, including gastroesophageal adenocarcinoma. However, our work, together with the work of Birocchi et al.[30], demonstrates the importance of balancing efficacy and on-target/off-tumor toxicity when targeting CLDN18.2.

On-target/off-tumor toxicity, while varying in penetrance and severity, appears to occur agnostic of the therapeutic format. We show here both the gross and histopathological evidence of gastric tissue injury correlating to the reported primary, treatment-emergent adverse events in zolbetuximab-treated patients, report on the frequency of such findings, and link clinical phenotype to pathological tissue injury. Reporting from patients treated with CT041 showed similar rates of gastrointestinal adverse events; while a small initial cohort of patients treated with LB1908 CLND18.2-CAR T cells demonstrated 50% grade ≧3 "gastritis/gastric mucosal injury," including a DLT[24]. In these trials, erosive gastritis was reported, which we demonstrated here in zolbetuximab-treated patients, but also mucosal lesions, perforation, and hemorrhage, which could potentially be related to on-target/off-tumor toxicity as well. Thus, on-target/off-tumor toxicity potentially limits the dose and therapeutic window of highly potent CLDN18.2-target therapies. Through the use of a mouse model that recapitulates the clinical phenomenon of on-target/off-tumor toxicity, we also demonstrated pathological injury resulting from treatment with CT041-scFv CAR T cells in a similar pattern to what we document clinically for zolbetuximab.

For CT041-scFv CAR T cells, this toxicity appears to be dependent on cell dose. Tumor burden-driven activation was not required to induce toxicity, as even in non-tumor-bearing animals, exposure to endogenous gastric mucosal CLDN18.2 was sufficient to lead to CAR T cell activation resulting in fatal on-target/off-tumor toxicity in all animals treated. While lowering the dose did mitigate toxicity, even a small dose de-escalation resulted in loss of tumor control in tumor-bearing animals, highlighting that a meaningful therapeutic window was challenging to identify. While our in vivo work used a 4-1BB co-stimulatory domain across all our CAR constructs, this second-generation format was also tested in vitro during CT041 pre-clinical development, but ultimately, due to slightly higher in vitro cytotoxicity, the CD28 co-stimulatory domain containing construct was selected for further investigation[26]. The work by Birocchi et al.[30] directly comparing the two designs in vivo demonstrates that toxicity is equally evident with CT041-scFv CAR T cells containing either commonly used co-stimulatory domain.

Many factors other than the co-stimulatory domain contribute to CAR activity. The 5795-VH-only binder has ~10× lower binding affinity than the 5797-VH and the CT041-scFv, and also substantially mitigates on-target/off-tumor toxicity while preserving anti-tumor efficacy. Mao et al. reviewed data from clinical trials of CAR T cell therapy in solid tumors and found that while many had high-affinity ($K_D < 20$ nM) antigen-binding domains, this did not correlate with the best clinical performance. Indeed, moderate affinity (K_D 20–100 nM) binders appeared to be more effective[31]. They also suggest that this may be an advantage in avoiding on-target/off-tumor toxicity as it allows discrimination between antigen^{high} tumors and antigen^{low} normal tissue. In general, the antigen density of CLDN18.2 in gastric tumors may be similar to expression levels in normal gastric mucosa[28], and it is thought that the dysregulation of localization to the tight junction in malignant transition may drive increased CLDN18.2 availability. It is possible that the tight junction architecture may present enough physical impediment to a lower-affinity CAR, whereas a high-affinity CAR can overcome this barrier, essentially erasing any antigen density gradient caused by this physical epitope exclusion in normal tissue. Affinity alone, however, may not completely explain the differences in therapeutic window. We also demonstrated that CT041-scFv and 5795-VH binding interactions with CLDN18.2 depend on a slightly different set of amino acids. This difference in binding epitope or geometry may also impact differential cytotoxicity in dysregulated (tumor) vs physiologic tight-junction (gastric) CLDN18.2 expression. Interestingly, the 5797-VH-only binder has a very similar binding affinity to the CT041-scFv and similar amino acid interactions as 5795. It has less toxicity than CT041-scFv CAR (although certainly more than 5795). This suggests that while affinity does modulate on-target/off-tumor toxicity, other attributes of the CAR mediated by the binder selection likely also contribute to determining toxic potential.

Other engineering approaches, in addition to affinity, can also be leveraged to address the on-target/off-tumor potential of antigens with essential normal tissue expression. "AND," or "IF>BETTER" logic gating can be used to pair two antigens expressed by different normal tissues or cell types if the malignant cells express both[32,33]. Proof of concept of CLDN18.2 "AND" logic partnering with MSLN is described in Birocchi et al.[30]. Tissue specificity, such as "IF>THEN,"[34] gating can be engineered to address non-gastric metastases. A trial design consisting of repeat administration of lower dose CLDN18.2-targeted CAR T cells is a non-genetic engineering approach that may also be explored to address enhancing the therapeutic window. The therapeutic window may also be addressed on the efficacy side by "armoring" a low-affinity CAR with an additional payload that enhances proliferation but does not lower the cytotoxic threshold.

Overall, these findings demonstrate the importance of on-target/off-tumor toxicity evaluation in pre-clinical development of targeted therapies to identify candidates with the potential for the largest therapeutic window. Further, as far as engineering CARs for solid tumors where antigens are often shared between malignant and normal tissue, distinguishable by a gradient in density or accessibility, this data provides further evidence that moderate affinity binding domains may be prioritized for incorporation into CAR designs for clinical translation.

Methods

Endoscopic image collection

Analysis included patients treated with chemotherapy plus zolbetuximab in the National Cancer Center Hospital East (Kashiwa, Japan) until September 2024. Patients who had provided written informed consent were prospectively enrolled in the biomarker study; it was reviewed and approved by the Institutional Review Boards (UMIN000019129). Chemotherapy plus zolbetuximab was given as standard of care, similar to the study protocol reported previously[18].

Hematoxylin and eosin (H&E) staining

Tissue sections were cut from formalin-fixed, paraffin-embedded blocks, and the first slide was used for H&E staining. Slides were

baked at 60 °C for 1 h, deparaffinized in three changes of xylene (2 min each), and rehydrated through graded ethanol (three changes of 100% ethanol for 2 min each, followed by 95% ethanol for 1 min, and distilled water for 5 min). Slides were stained with hematoxylin for 5 s, rinsed in water, treated with a bluing reagent for 30 s, and rinsed again. Eosin staining was performed for 15 s. Slides were then dehydrated in three changes of 100% ethanol and cleared in three changes of xylene (2 min each), followed by coverslipping with a permanent mounting medium.

Multiplex immunofluorescence (mIF)

To evaluate changes in T cell infiltration and CLDN18.2 expression, a customized mIF panel was developed. The panel included monoclonal antibodies targeting CLDN18.2, a tight junction cell surface marker, CD3, a T cell marker, pan-cytokeratin (pan-CK), to distinguish epithelial cells, and the DNA-binding dye 2-(4-amidinophenyl)-1H-indole-6-carboxamidine (DAPI) as a nuclear marker.

Staining conditions for each antibody were optimized using immunohistochemistry (IHC) and singleplex immunofluorescence using one Opal fluorophore and DAPI to assess signal intensity, localization, and spectral separation. Following optimization, all antibodies were combined into a single mIF assay. Multiplex staining was performed on a Leica BOND RX Research Stainer (Leica Biosystems) using sequential rounds of antigen retrieval, primary antibody incubation, HRP-conjugated secondary detection, and fluorophore labeling via tyramide signal amplification.

Summary of primary antibodies and Opal fluorophores used in the mIF assay, see Supplementary Table 1.

Multispectral images were captured on the PhenoImager HT multispectral imaging system (Akoya Biosciences, Hopkinton, MA). A 10× overview scan was performed, followed by high-resolution imaging at 20× magnification for selected regions of interest (ROIs). Spectral unmixing and fluorophore separation were conducted using inForm 3.0.0 software (Akoya Biosciences), and unmixed images were exported for analysis. Unmixed images were imported into QuPath v0.5.1 (open-source software available on GitHub). Adjacent ROIs were aligned and merged to generate high-resolution composite images, enabling comprehensive visualization of marker expression across larger tissue areas for spatial analysis and interpretation

Cells

OE19 and PATU8988s cell lines were acquired from the DSMZ collection (Braunschweig, Germany) and were cultured according to the manufacturer's recommendation. They were tested monthly for Mycoplasma using PCR (Bulldog Bio). Human blood was procured from the Harvard Crimson Core as deidentified, discarded blood donations from consenting donors. Human peripheral blood mononuclear cells (PBMCs) isolated by ficoll density centrifugation or purified T cells (RosetteSep Human T Cell Enrichment Cocktail, StemCell #15061) were stimulated with TransAct (Miltenyi), 10 μL for 5e6 PBMCs/mL or for 1e6 T cells/mL, in complete RPMI medium: RPMI (Gibco #118750-093) supplemented with 10% heat inactivated Fetal Bovine Serum (FBS) (Life Technologies #10438026), Penicillin-Streptomycin (P/S) (Life Technologies #15140122), Glutamax (GX) (Life Technologies #35050061). The human recombinant cytokines IL-2 (200 U/mL final), IL-7 (5 ng/mL final) and IL-15 (10 ng/mL final) were added.

To generate cell lines overexpressing chimeric CLDN18.1/18.2 constructs, HEK293s (ATCC, Manassas, VA, USA) were engineered to overexpress chimeric CLDN18 using lentiviral constructs for the CMV-driven expression of each construct (i.e., ECL1-1, 1-2, 1-3) as well as a puromycin marker for selection. Since the two isoforms only differ in 5 distinctly extracellular amino acids centered in three structurally distinct regions, each chimeric construct harbored 1 or 2 mutations in the ECL. ECL1-1 mutations (N45Q and Q47E) centered on the unstructured, N-terminus of the pore-lining loop, ECL1-2 mutations (N37D and A42S) near the "GLW" signature sequence within the β-fold of the loop, and ECL1-3 (E56Q) formed by the residues sandwiched within the disulfide bond in the loop Transduced HEK293s overexpressing chimeric constructs were selected with 1.25 μg/mL puromycin (Thermo Fisher Scientific, Waltham, MA #A1113803) for 5–7 days prior to inclusion in cytotoxicity assays.

Luciferase-based cytotoxicity

SNU1s overexpressing domain-specific constructs were made GFP/luciferase positive by stably transducing with gamma retrovirus expressing the cDNA as described previously (Smith et al.[35]). 10,000 of these target cells were plated in 96-well plates in triplicate with CAR+ T cells at the indicated effector-to-target (E:T) ratios; cells were then incubated for 72 h. Cell viability was determined by a luciferase-dependent assay with OneGlo substrate E6110 (Promega Madison, WI, USA), where % cytotoxicity = (BLI Control− BLISAMPLE)/BLIMAX; BLI Control = mean target cell alone value of that experiment with a non-targeting control (12). Bioluminescence was read on an Agilent Cytation5 5 (Santa Clara, CA, USA).

Binder discovery

HCAb Harbour Mice® (Version 2.1) were immunized with HEK293 cells overexpressing human CLDN18.2. B cells and plasma cells from the blood, spleen, and marrow were obtained, and specific and productive VH-secreting cells were identified through SBC (Single B Cell) screening on the Beacon optofluidic system, single B/plasma cell sequencing, followed by confirmation using 24-well transient transfection supernatants to generate bivalent VH-Fc format binders. These were purified via size exclusion chromatography by HPLC and screened for binding affinity and specificity via flow cytometry against CHO-K1 cells engineered to express either human CLDN18.2 (positive binding) or human CLDN18.1 (negative for binding). Binding was further confirmed in cell lines that endogenously express CLDN18.2, NUGC4_D8 cells, and SNU620 cells (SNU620 has an M149L mutation).

CAR construct

A modified version of a third-generation self-inactivating (SIN) lentiviral CMV-GFP-WPRE transfer plasmid (Addgene 17446, PGK-HygroR cassette removed) was used as an acceptor vector to clone candidate CAR sequences. CAR including CMV promoter, binder, CD28 hinge and transmembrane domain, 4-1BB co-stimulatory domain, and a CD3ζ activation domain was incorporated, along with vexGFP reporter. For sequences, see Supplementary Table 2.

Binding kinetics of CLDN18.2-targeting human VH binders

SPR experiments were done on the Nicoya AltoSPR using PBS supplemented with 1% BSA and 0.1% Tween 20 running buffer (Nicoya Lifesciences PBS-T, Kitchener, ON, Canada). To generate a capture surface, Protein A (Nicoya Lifesciences ALTO-R-PROA-KIT) diluted in a sodium acetate buffer, pH 5.0, was amine-coupled to the sensor surface of a 16-channel carboxyl cartridge (Nicoya Lifesciences KC-CBX-PEG-16) via EDC and NHS. For kinetics experiments, two anti-CLDN18.2 heavy chain only antibodies (HCAbs), previously generated in-house by Harbour BioMed and single-step purified by Protein A, as well as a custom-produced CT041 IgG1 antibody (WuXi Biologics, Shanghai, China), and an irrelevantly targeted IgG control were diluted to 10 μg/mL in running buffer and individually captured on sensor surfaces previously immobilized with Protein A. Recombinant human CLDN18.2-his (Genscript Z03504-10, Piscataway, NJ, USA) was diluted to 1800 nM in running buffer and then serially diluted 3-fold for a total of five concentrations as well as a baseline control sample at 0 nM. Each dilution of rhCLDN 18.2 was flowed over the captured antibodies from low to high concentration with a regeneration of 10 mM glycine-HCl pH 1.5 (Nicoya Lifesciences ALTO-R-GLYHCl-1.5) in between each cycle. Resulting sensorgrams were double referenced and, where

applicable, fit to a 1:1 Langmuir binding model. All k_{on}s, k_{off} s, and K_Ds are reported as mean ± standard deviation from a total of four separate experiments.

CAR T cell production

Lenti-X 293T cells (Takara) were seeded at 50,000 cells/cm^2 the day before transfection using TransIT-293 Transfection Reagent (Mirus). The relative amounts of plasmids for a 15 cm plate (145 cm^2) were as follows: Packaging psPAX2 (Gag-Pol-Rev-Tat, Addgene 12260): 3 pmol, envelop pMD2.G (VSVg, Addgene 12259): 1.6 pmol, PKR inhibitor (pAdv, Promega #E1711): 0.9 pmol, transfer: 3.7 pmol. For other types of plates, the amounts of plasmids were adjusted proportionally to the surface. The media was changed with fresh media 24 h post-transfection. The viral supernatant was harvested 48 h post-transfection. Viral supernatants were cleared from debris after centrifugation (500 g, 5 min, 4 °C) followed by 0.45 μm filtration. Viral supernatants were used directly for transduction or concentrated by ultracentrifugation (110,000 × *g*, 2 h, 4 °C), aliquoted, and stored at −80 °C. Deidentified, discarded blood from donors was used for the isolation of immune cells for the production of CAR T cells. The Harvard Crimson Core is responsible for the collection and distribution of these products from the platelet donation center at MGH. T cells were prepared and activated as above. After at least 2 days, cells were transduced with lentivirus via spinoculation (2000 × *g*, 1 h, 30 °C), monitored daily, and kept at 0.5-1e6 cells/mL. Transduction efficiency could be enhanced using 1 mg/mL Poloxamer 338 (P338) (Sigma Aldrich #P2164021). vexGFP expression was measured to determine transduction efficiency in each CAR T cell batch 5–6 days after transduction by flow cytometry analysis using the 2 (V-B) or 3-laser (V-B-R) Northern Lights and SpectroFlo software (Cytek) (Supplementary Fig. 10). Prior to injection, cells were normalized to the lowest transduction efficiency by adding mock transduced T cells from the same donor, such that each experimental group received the same number of CAR+ T cells and also the total number of T cells.

In vivo models

NSG-DKO mice (JAX strain #025216) were purchased from The Jackson Laboratory (Bar Harbor, ME, USA). Animals were allowed to acclimate for at least 7 days before initiation of a study. The in vivo studies were conducted at Dana-Farber Cancer Institute with the prior approval of the Institutional Animal Care and Use Committee (IACUC, protocol numbers 20-010 and 16-015) in an AAALAC-accredited vivarium with a standard 12 h dark/12 h light cycle under controlled environmental conditions (temperature: 20 ± 2 °C; humidity: 35 ± 10%). Xenografts were produced as follows: 4×10^6 cells were resuspended with 50% Matrigel (Corning) and were implanted subcutaneously in the flank of 6–8-week-old NSG-DKO mice. Tumors were allowed to establish, and animals were grouped to normalize tumor volume prior to a single IV injection of either control αBCMA CAR T or αCLDN18.2 CAR T cells. Tumors were measured with a caliper, and volumes were determined using the formula, Tumor volume = (length × width^2)/2. Tumor volumes and body weights were measured weekly. Body weight loss of 80% from baseline and tumor volumes >2000 mm^3 were humane endpoints on study; any animals plotted reached these values were sacrificed accordingly.

Statistical methods

Analyses were performed with GraphPad Prism 10 (version 10.4). Tests used are indicated in the corresponding figure legends. Significance was considered for two-sided $P < 0.05$ as the following: p = *<0.05, **<0.01, ***<0.001, ****<0.0001.

Reporting summary

Further information on research design is available in the Nature Portfolio Reporting Summary linked to this article.

Data availability

The data generated for this study are available within the article, Supplementary Information, or Source data file. Source data are provided with this paper.

References

1. Sung, H. et al. Global Cancer Statistics 2020: GLOBOCAN Estimates of Incidence and Mortality Worldwide for 36 Cancers in 185 Countries. *CA Cancer J. Clin.* **71**, 209–249 (2021).
2. Ferlay, J. et al. Cancer statistics for the year 2020: an overview. *Int. J. Cancer* **149**, 778–789 (2021).
3. Rha, S. Y. et al. Pembrolizumab plus chemotherapy versus placebo plus chemotherapy for HER2-negative advanced gastric cancer (KEYNOTE-859): a multicentre, randomised, double-blind, phase 3 trial. *Lancet Oncol.* **24**, 1181–1195 (2023).
4. Janjigian, Y. Y. et al. 1400O Final overall survival for the phase III, KEYNOTE-811 study of pembrolizumab plus trastuzumab and chemotherapy for HER2+ advanced, unresectable or metastatic G/GEJ adenocarcinoma. *Ann. Oncol.* **35**, S877–S878 (2024).
5. Janjigian, Y. Y. et al. First-line nivolumab plus chemotherapy for advanced gastric, gastroesophageal junction, and esophageal adenocarcinoma: 3-year follow-up of the phase III CheckMate 649 trial. *J. Clin. Oncol.* **42**, 2012–2020 (2024).
6. Choi, E., Shin, J., Ryu, M. H., Kim, H. D. & Park, Y. S. Heterogeneity of claudin 18.2 expression in metastatic gastric cancer. *Sci. Rep.* **14**, 1–9 (2024).
7. Klempner, S. J., Janjigian, Y. Y. & Wainberg, Z. A. Claudin18.who? Examining biomarker overlap and outcomes in claudin18.2-positive gastroesophageal adenocarcinomas. *ESMO Open* **8**, 100778 (2023).
8. Shitara, K. et al. Global prevalence of claudin 18 isoform 2 in tumors of patients with locally advanced unresectable or metastatic gastric or gastroesophageal junction adenocarcinoma. *Gastric Cancer* **27**, 1058 (2024).
9. Kim, H. D. et al. Clinicopathologic features and prognostic value of claudin 18.2 overexpression in patients with resectable gastric cancer. *Sci. Rep.* **13**, 20047 (2023).
10. Niimi, T. et al. claudin-18, a novel downstream target gene for the T/EBP/NKX2.1 homeodomain transcription factor, encodes lung- and stomach-specific isoforms through alternative splicing. *Mol. Cell. Biol.* **21**, 7380–7390 (2001).
11. Sahin, U. et al. Claudin-18 Splice Variant 2 is a pan-cancer target suitable for therapeutic antibody development. *Clin. Cancer Res.* **14**, 7624–7634 (2008).
12. Türeci, Ö, Mitnacht-Kraus, R., Wöll, S., Yamada, T. & Sahin, U. Characterization of zolbetuximab in pancreatic cancer models. *Oncoimmunology* **8**, e1523096 (2018).
13. Moentenich, V. et al. Claudin 18.2 expression in esophageal adenocarcinoma and its potential impact on future treatment strategies. *Oncol. Lett.* **19**, 3665 (2020).
14. Wagner, P. et al. Spatial expression of claudin 18.2 in matched primaries and metastases of tubo-ovarian carcinoma of all subtypes. *Virchows Arch.* **485**, 63 (2024).
15. Micke, P. et al. Aberrantly activated claudin 6 and 18.2 as potential therapy targets in non-small-cell lung cancer. *Int. J. Cancer* **135**, 2206–2214 (2014).
16. Shitara, K. et al. Zolbetuximab plus mFOLFOX6 in patients with CLDN18.2-positive, HER2-negative, untreated, locally advanced unresectable or metastatic gastric or gastro-oesophageal junction adenocarcinoma (SPOTLIGHT): a multicentre, randomised, double-blind, phase 3 trial. *Lancet* **401**, 1655–1668 (2023).
17. Shah, M. A. et al. Zolbetuximab plus CAPOX in CLDN18.2-positive gastric or gastroesophageal junction adenocarcinoma: the randomized, phase 3 GLOW trial. *Nat. Med.* **29**, 2133–2141 (2023).

18. Shitara, K. et al. Zolbetuximab in gastric or gastroesophageal junction adenocarcinoma. *N. Engl. J. Med.* **391**, 1159–1162 (2024).
19. Xu, Q., Jia, C., Ou, Y., Zeng, C. & Jia, Y. Dark horse target Claudin18.2 opens new battlefield for pancreatic cancer. *Front. Oncol.* **14**, 1371421 (2024).
20. Xu, G. et al. CMG901, a Claudin18.2-specific antibody-drug conjugate, for the treatment of solid tumors. *Cell Rep. Med.* **5**, 101710 (2024).
21. Qi, C. et al. Claudin18.2-specific CAR T cells in gastrointestinal cancers: phase 1 trial final results. *Nat. Med.* **30**, 2224–2234 (2024).
22. Botta, G. P. et al. Multicenter phase Ib trial in the U.S. of salvage CT041 CLDN18.2-specific chimeric antigen receptor T-cell therapy for patients with advanced gastric and pancreatic adenocarcinoma. *J. Clin. Oncol.* **40**, 2538–2538 (2022).
23. Qi, C. et al. Claudin-18 isoform 2-specific CAR T-cell therapy (satricel) versus treatment of physician's choice for previously treated advanced gastric or gastro-oesophageal junction cancer (CT041-ST-01): a randomised, open-label, phase 2 trial. *Lancet* **405**, 2049–2060 (2025).
24. Zhen, D. B. et al. Preliminary results of a phase 1 study of LB1908, an autologous Claudin 18.2–targeted chimeric antigen receptor T-cell product, in patients with advanced gastroesophageal adenocarcinoma. *J. Clin. Oncol.* **43**, 4022–4022 (2025).
25. Türeci, Ö et al. Claudin-18 gene structure, regulation, and expression is evolutionary conserved in mammals. *Gene* **481**, 83–92 (2011).
26. Jiang, H. et al. Claudin18.2-specific chimeric antigen receptor engineered T cells for the treatment of gastric cancer. *J. Natl. Cancer Inst.* **111**, 409–418 (2019).
27. Brehm, M. A. et al. Lack of acute xenogeneic graft-versus-host disease, but retention of T-cell function following engraftment of human peripheral blood mononuclear cells in NSG mice deficient in MHC class I and II expression. *FASEB J.* **33**, 3137–3151 (2019).
28. Mathias-Machado, M. C. et al. Claudin 18.2 as a New Biomarker in Gastric Cancer—What Should We Know? *Cancers* **16**, 679 (2024).
29. Drabek, D. et al. Expression cloning and production of human heavy-chain-only antibodies from murine transgenic plasma cells. *Front. Immunol.* **7**, 232393 (2016).
30. Birocchi, F. et al. On-target off-tumor toxicity of Claudin18.2-directed CAR-T cells in preclinical models. *Nat. Commun.* (2025).
31. Mao, R., Kong, W. & He, Y. The affinity of antigen-binding domain on the antitumor efficacy of CAR T cells: moderate is better. *Front. Immunol.* **13**, 1032403 (2022).
32. Tousley, A. M. et al. Co-opting signalling molecules enables logic-gated control of CAR T cells. *Nature* **615**, 507 (2023).
33. Haubner, S. et al. Cooperative CAR targeting to selectively eliminate AML and minimize escape. *Cancer Cell* **41**, 1871–1891.e6 (2023).
34. Roybal, K. T. et al. Engineering T cells with customized therapeutic response programs using synthetic notch receptors. *Cell* **167**, 419–432.e16 (2016).
35. Smith, E. L. et al. Development and Evaluation of an Optimal Human Single-Chain Variable Fragment-Derived BCMA-Targeted CAR T Cell Vector. *Mol. Ther.* **26**, 1447–1456 (2018).

Acknowledgements

E.J.C. is supported by the Lubin Family Foundation Scholar Award. E.L.S. receives research support from the DeGregorio Family Foundation, Torrey Coast, Parker Institute for Cancer Immunotherapy, Massachusetts Life Sciences Center, and the Lavine Family. The Dana-Farber/Harvard Cancer Center (DF/HCC) is supported in part by the NCI Cancer Center Support Grant P30CA006516. A.J.A. is funded by Break Through Cancer, the Lustgarten Foundation, the Pancreatic Cancer Action Network, NIH-NCI P50CA127003, U01 CA274276, R01 CA276268, the DeGregorio Family Foundation and the Dana-Farber Cancer Institute Hale Center for Pancreatic Cancer Research. S.J.K. DeGregorio Family Foundation, The Torrey Coast Foundation, Gastric Cancer Foundation Seed Grant and the GI-SPORE P50CA127003. J.A.N. receives research support from the DeGregorio Family Foundation and Natera. The authors thank Timothy Haggerty for help with Biorender figure preparation.

Author contributions

Clinical data were collected and interpreted by K.S., I.N., S.J.K. and N.S.; antibody discovery was performed by Q.L., J.Z., C.N., C.D., X.W. and L.L.; pre-clinical models and CAR T cells were conceived of by E.L.S., A.A. A.R., K.T. and E.J.C and these experiments were executed and analyzed by K.T., E.J.C., S.N., M.D.V., A.M. and A.R. Histology and mIF was designed, performed and analyzed by J.A.N and M.M. E.J.C., C.H.N., T.W., S.J.K., A.A. and E.L.S. prepared the manuscript and it was reviewed by all authors. A.R., J.A.N., K.S., A.A. and E.L.S. supervised the work.

Competing interests

E.L.S. has consulted for ArsenalBio, Blackstone Life Sciences, Chroma Medicine, Clade Therapeutics, Eureka Therapeutics, ImmuneBridge, Legend Biotech, Overland Pharmaceuticals, Predicta Biosciences, and Sana Biotech. E.L.S. holds equity in Predicta Biosciences and receives research funding from Sanofi. E.L.S. is an inventor on licensed patents regarding CAR T cells and antibodies to treat multiple myeloma and received royalties from Bristol Myers Squibb and Sanofi. E.L.S. was on a Scientific Advisory Board for Bristol Myers Squibb, Chimeric Therapeutics, Novartis, and Sanofi. S.J.K has served a consultant/advisory role for Bristol Myers Squibb, Merck, Eli Lilly, Roche, Astellas, Daiichi Sankyo, Pieris, Natera, Novartis, AstraZeneca, Mersana, Sanofi-Aventis, Taiho Oncology, Eisai, and I-Mab Therapeutics. J.A.N. serves as a consultant for Leica Biosystems. A.J.A. has consulted for Anji Pharmaceuticals, Affini-T Therapeutics, Arrakis Therapeutics, AstraZeneca, Boehringer Ingelheim, Kestrel Therapeutics, Merck & Co., Inc., Mirati Therapeutics, Nimbus Therapeutics, Oncorus, Inc., Plexium, Quanta Therapeutics, Revolution Medicines, Reactive Biosciences, Riva Therapeutics, Servier Pharmaceuticals, Syros Pharmaceuticals, Taiho Pharmaceuticals, T-knife Therapeutics, Third Rock Ventures, and Ventus Therapeutics. A.J.A. holds equity in Riva Therapeutics and Kestrel Therapeutics. A.J.A. has received research funding from Amgen, AstraZeneca, Boehringer Ingelheim, Bristol Myers Squibb, Deerfield, Inc., Eli Lilly, Mirati Therapeutics, Nimbus Therapeutics, Novartis, Novo Ventures, Revolution Medicines, and Syros Pharmaceuticals. K.S. reports receiving fees for consulting and advisory roles from Bristol Myers Squibb, Takeda, Ono Pharmaceutical, Novartis, Daiichi Sankyo, Amgen, Boehringer Ingelheim, Merck Pharmaceutical, Astellas, Guardant Health Japan, Janssen, AstraZeneca, Zymeworks Biopharmaceuticals, ALX Oncology Inc, Bayer, GlaxoSmithKline, HEALIOS, Moderna Inc, Arcus Biosciences Inc; receiving honoraria from Bristol Myers Squibb, Janssen, AstraZeneca, Eli Lilly, Ono Pharmaceutical, and Astellas. K.S. has research funding from Merck Pharmaceutical, Daiichi Sankyo, Taiho Pharmaceutical, Chugai Pharma, Ono Pharmaceutical, Astellas, Eisai, Amgen, PRA Health Sciences, AstraZeneca, PPD-SNBL K.K., and TORAY. I.N. receives research funding from Astellas, Ono Pharmaceutical Co., Ltd., Merck Sharp & Dohme (MSD), Daiichi Sankyo, Boehringer Ingelheim, and Chugai Pharmaceutical Co., Ltd. Honoria from Astellas, Ono Pharmaceutical Co., Ltd., Bristol Myers Squibb, Merck Sharp & Dohme (MSD), Daiichi Sankyo, and Chugai Pharmaceutical Co., Ltd. N.S. received lecture fees from Astellas. A.R. has consulted for Black Opal Ventures (BOV). Q.L., J.Z., C.N., C.D., X.W., and L.L. are employees of Nona Biosciences (Suzhou) Co., Ltd.; E.L.S., E.J.C., A.R., Q.L., J.Z., C.N., C.D., X.W., and L.L. are inventors on the patent CLDN18 VH CAR, App. No. 202510028444.4 related to this work. K.T., M.D.V., M.M., S.K.N., A.M., C.H.N., and T.W. do not report any conflicts of interest.

Additional information

Supplementary information The online version contains supplementary material available at https://doi.org/10.1038/s41467-025-65148-6.

Correspondence and requests for materials should be addressed to Eric L. Smith.

Peer review information *Nature Communications* thanks Prasad Adusumilli, Yanping Yang, and the other, anonymous, reviewer(s) for their contribution to the peer review of this work. A peer review file is available.